Supporting Information for

Anion Capture at the Open Core of a Geometrically Flexible Dicopper(II,II) Macrocycle Complex

Sam H. Brooks, Corey A. Richards, Patrick J. Carroll, Michael R. Gau, and Neil C. Tomson*

Department of Chemistry, University of Pennsylvania, Philadelphia, Pennsylvania 19104, United States

** tomson@upenn.edu*

Table of Contents:

I. NMR Spectra

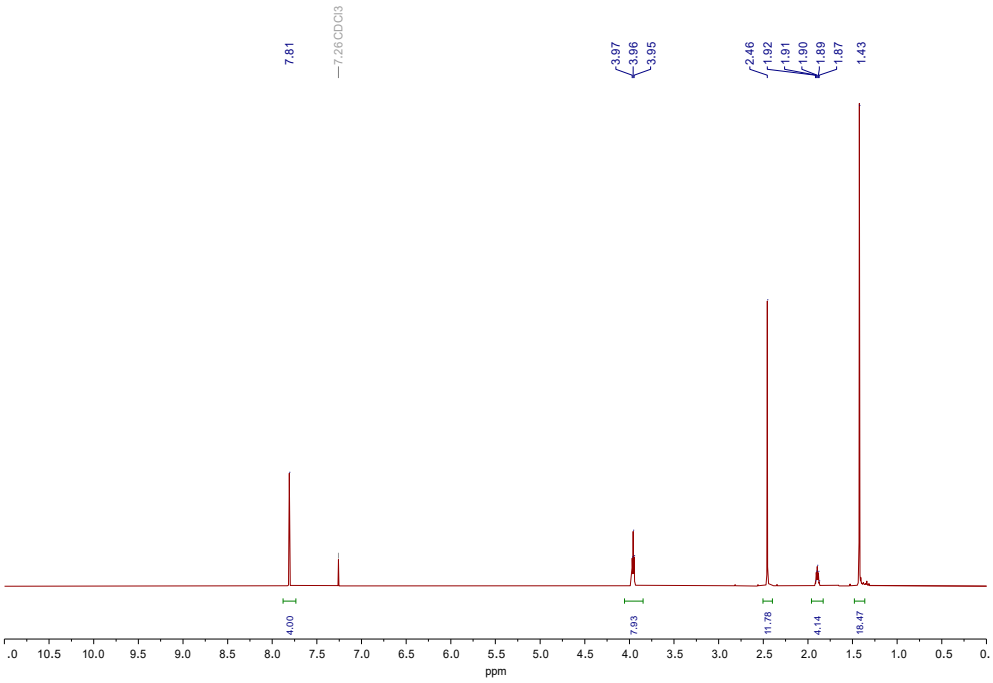

Figure S1 ^{1}H NMR spectrum of **^{3}[Sr]$^{2+}$** in $CDCl_3$.

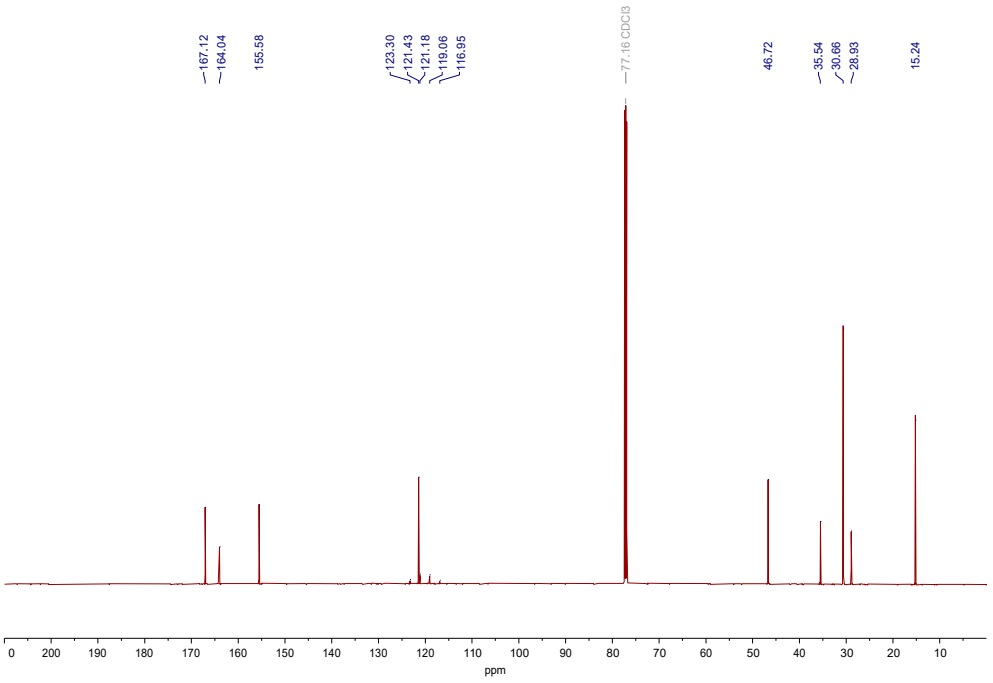

Figure S2 $^{13}C\{^{1}H\}$ NMR spectrum of **^{3}[Sr]$^{2+}$** in $CDCl_3$.

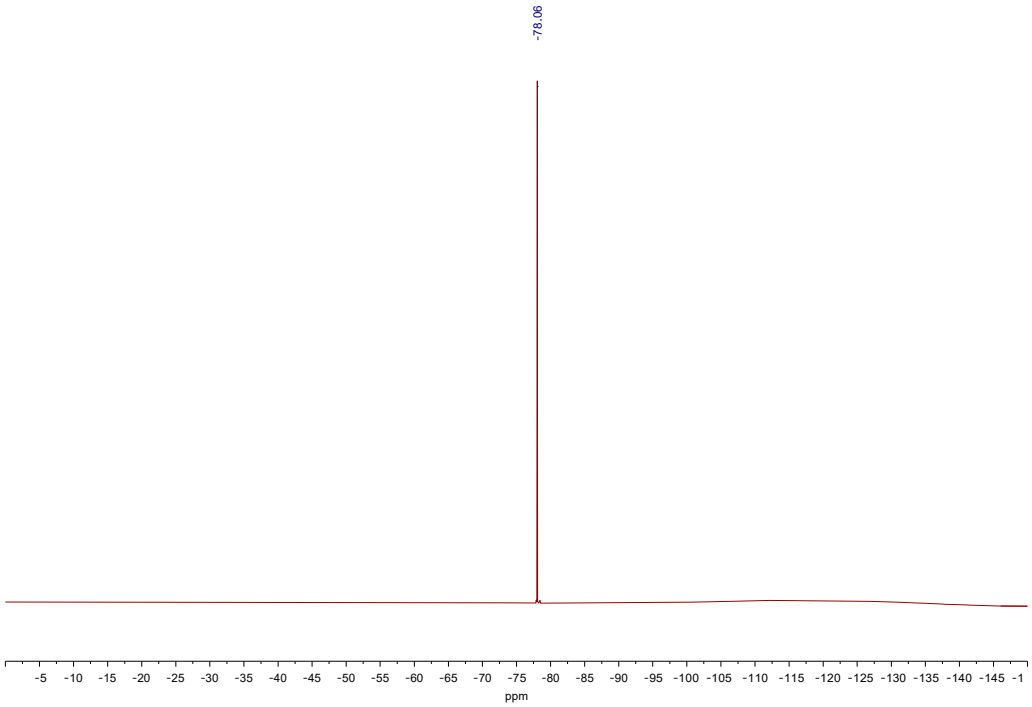

Figure S3 $^{19}F\{^{1}H\}$ NMR spectrum of **^{3}[Sr]$^{2+}$** in $CDCl_3$.

II. Infrared Spectra

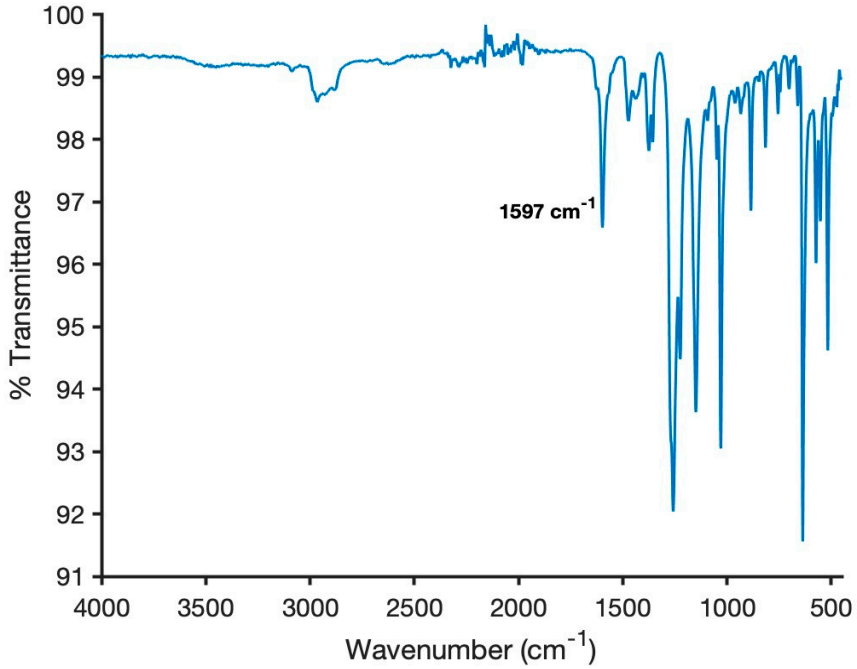

Figure S4 Infrared spectrum of $^{3}[Cu_2Cl_2]^{2+}$.

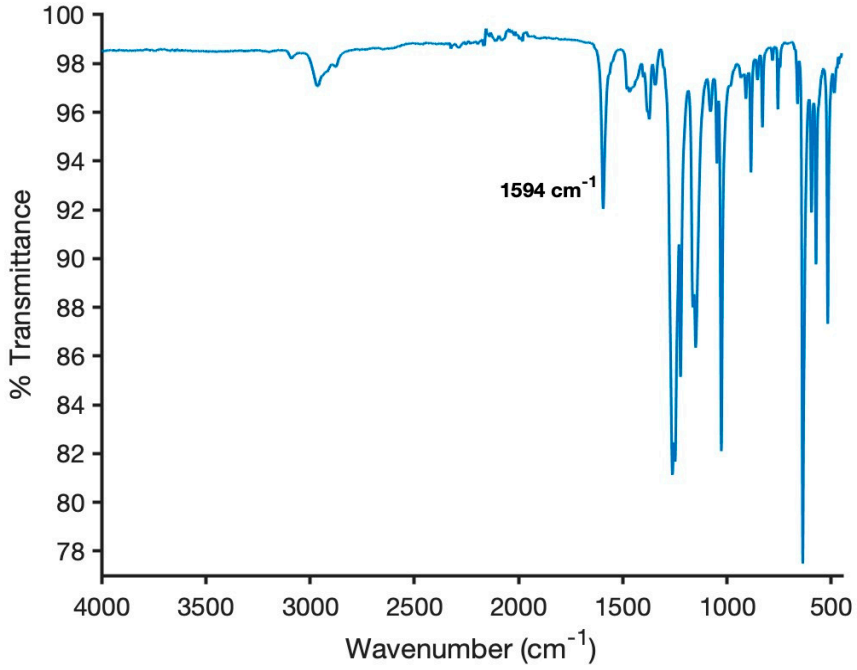

Figure S5 Infrared spectrum of $^{2}[Cu_2Cl_2]^{2+}$.

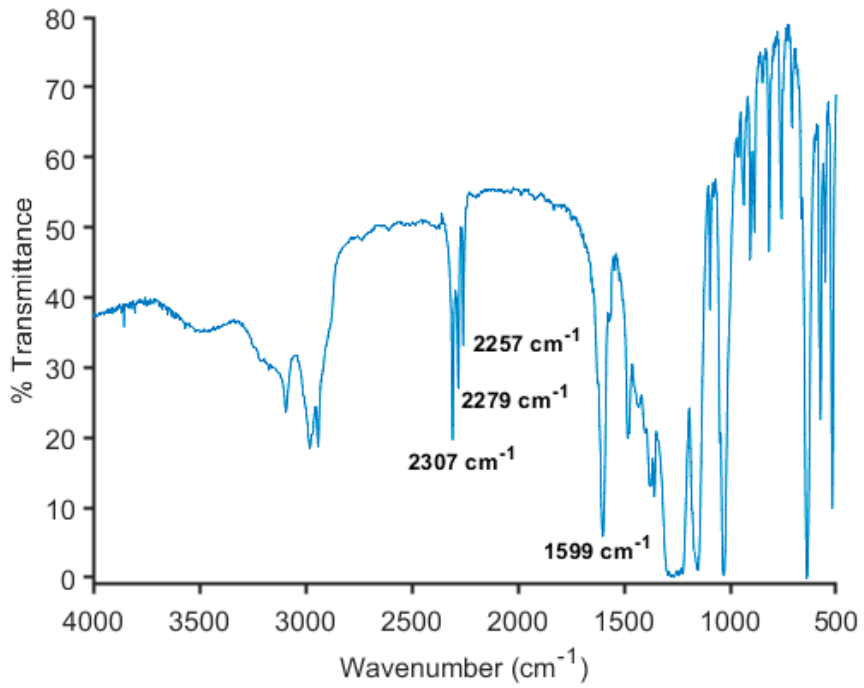

Figure S6 Infrared spectrum of $^{3}[Cu_2(NCMe)_2]^{4+}$.

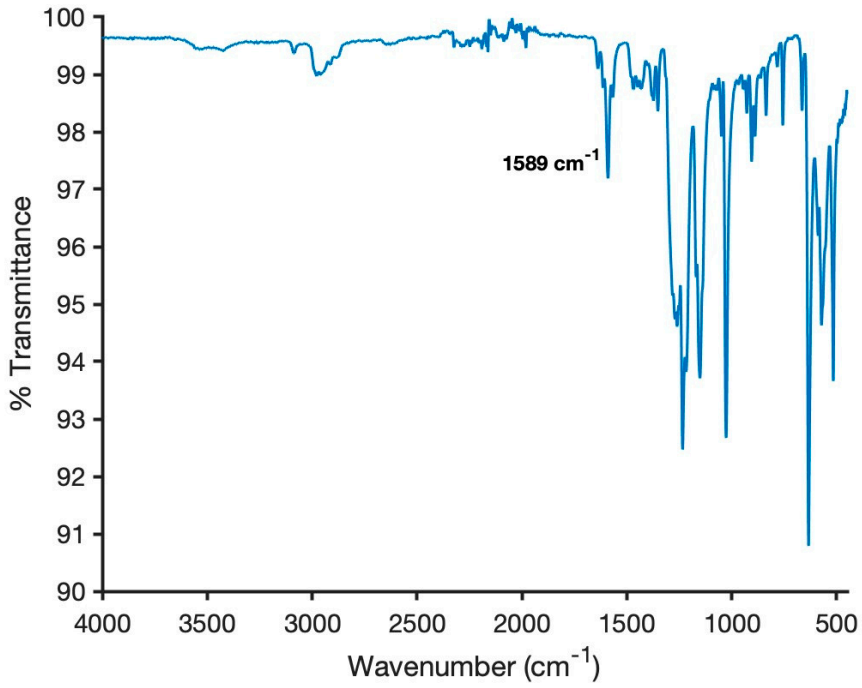

Figure S7 Infrared spectrum of $^{3}[Cu_2F]^{3+}$.

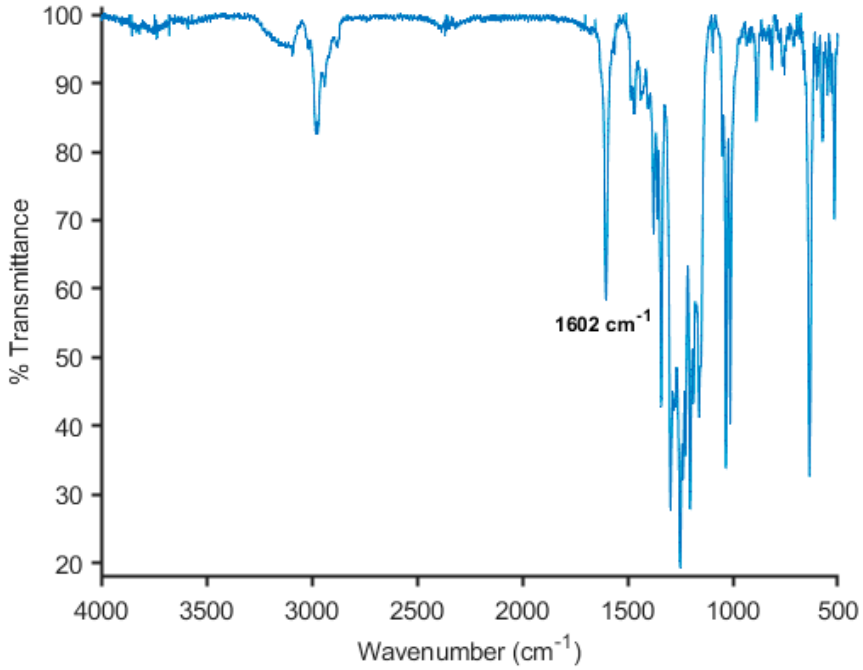

Figure S8 Infrared spectrum of $^{3}[Cu_2]^{4+}$.

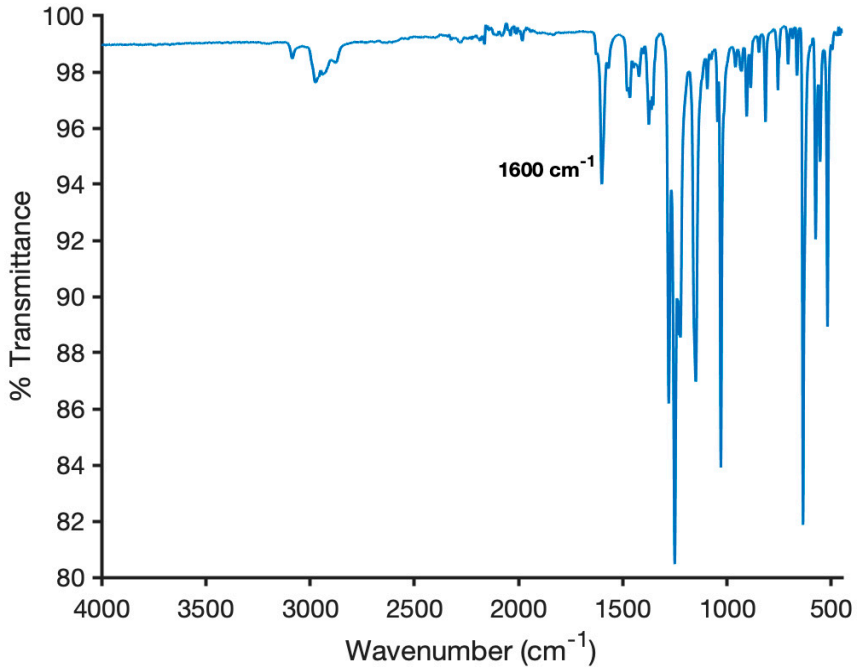

Figure S9 Infrared spectrum of $^{3}[Cu_2Br_2]^{2+}$.

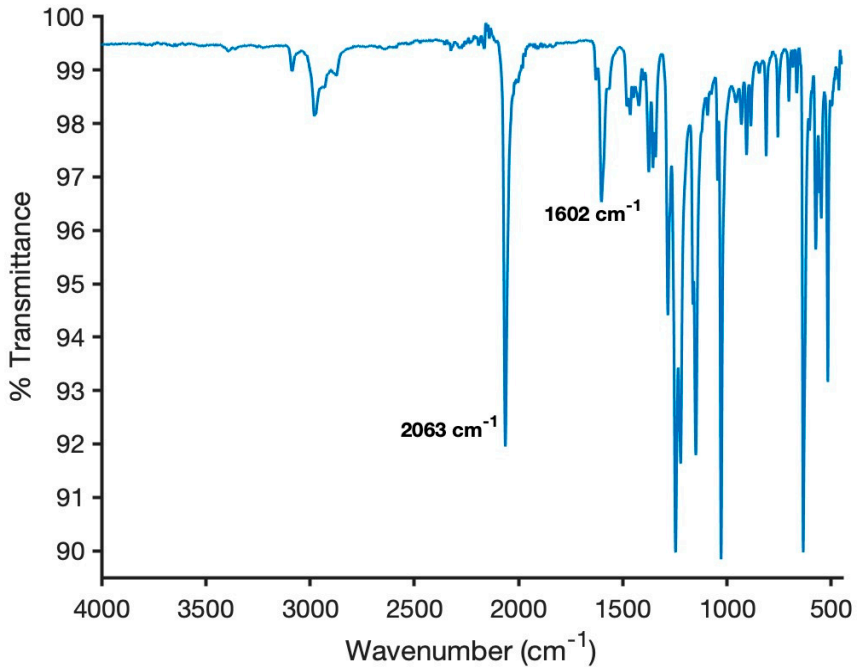

Figure S10 Infrared spectrum of $^{3}[Cu_2(N_3)_2]^{2+}$.

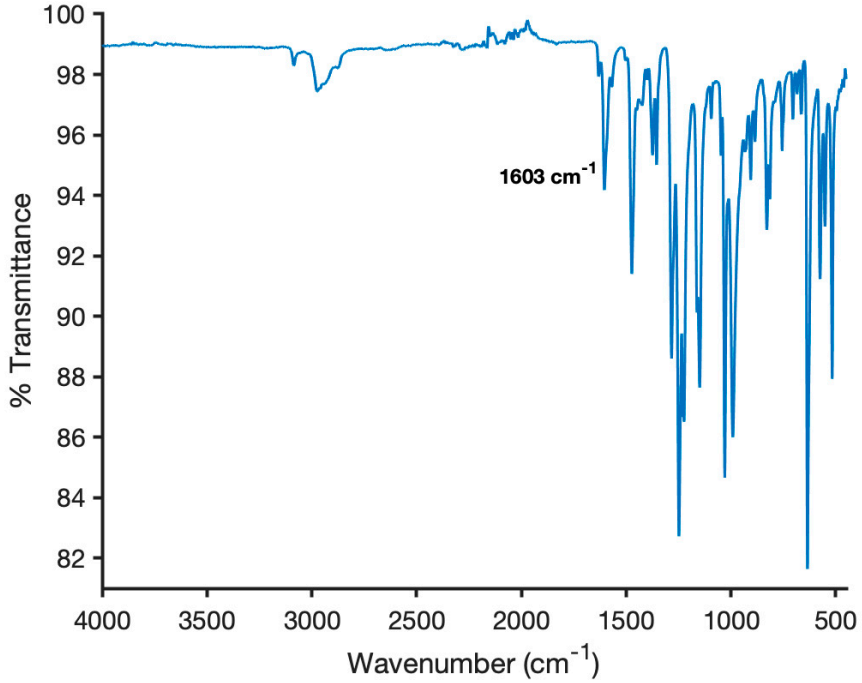

Figure S11 Infrared spectrum of $^{3}[Cu_2(ONO)_2]^{2+}$.

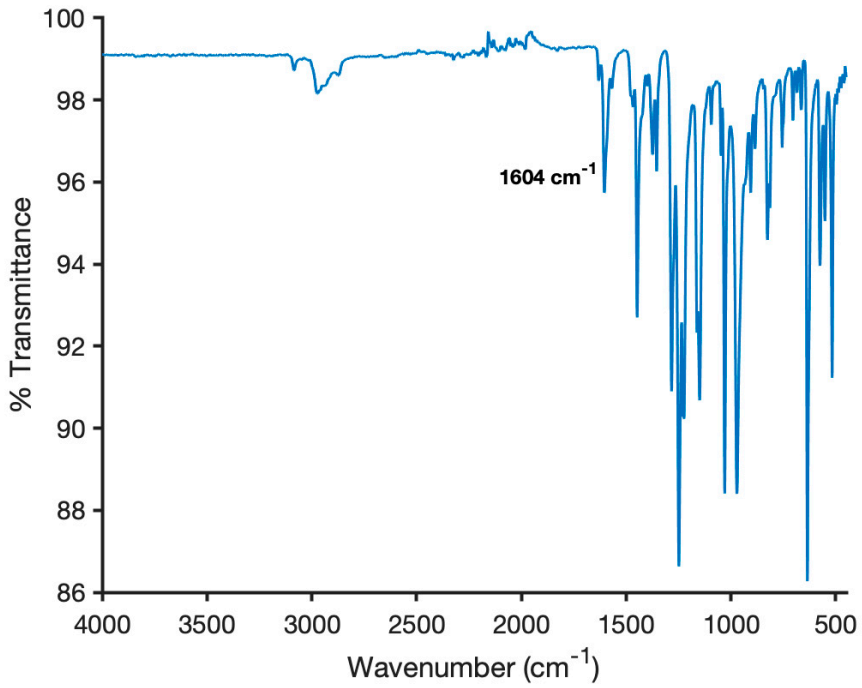

Figure S12 Infrared spectrum of $^{3}[Cu_2(O^{15}NO)_2]^{2+}$.

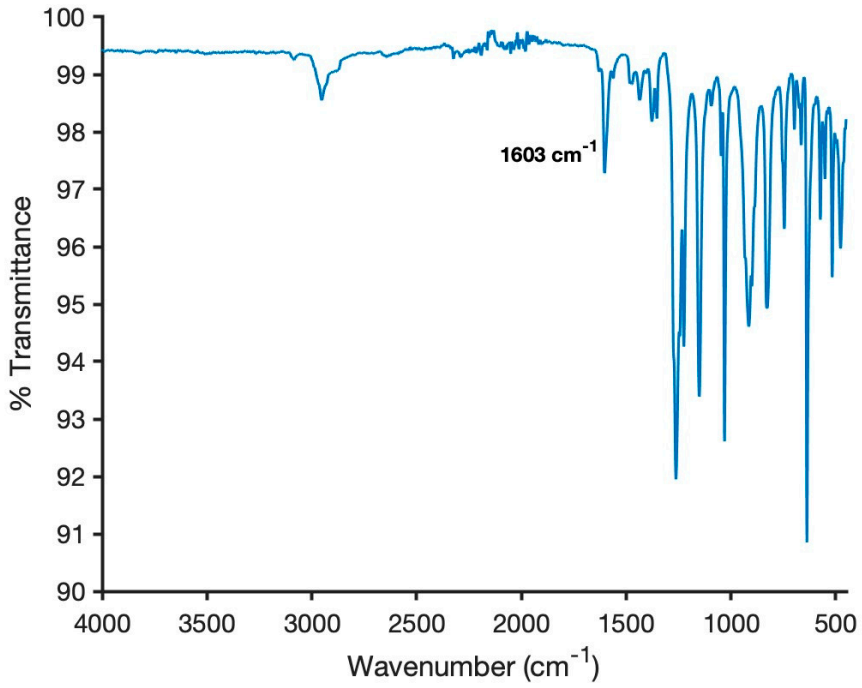

Figure S13 Infrared spectrum of $^{3}[Cu_2(OTMS)_2]^{2+}$.

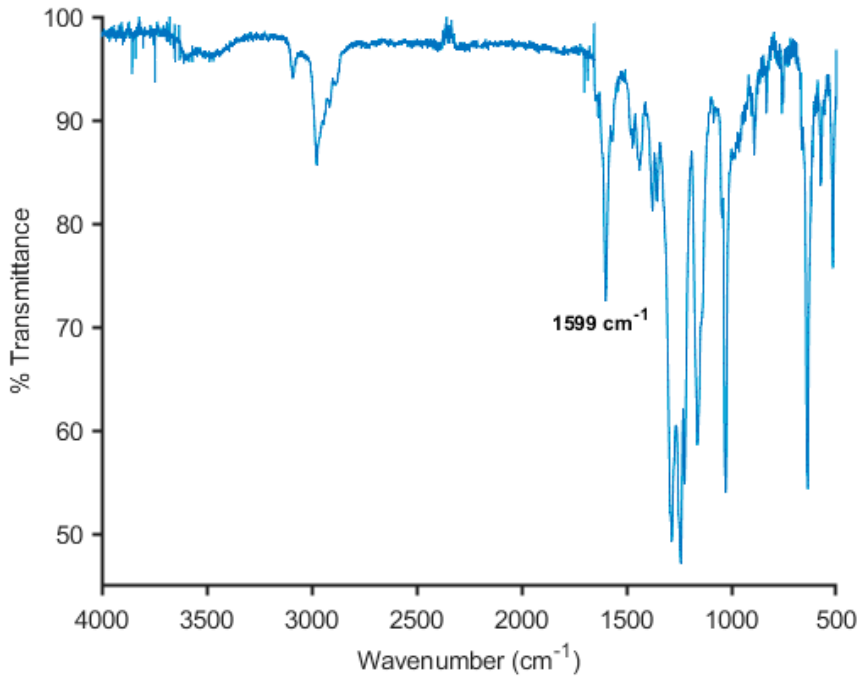

Figure S14 Infrared spectrum of ^{3}**[Cu$_2$OH]$^{3+}$**.

III. UV-vis-NIR Spectra

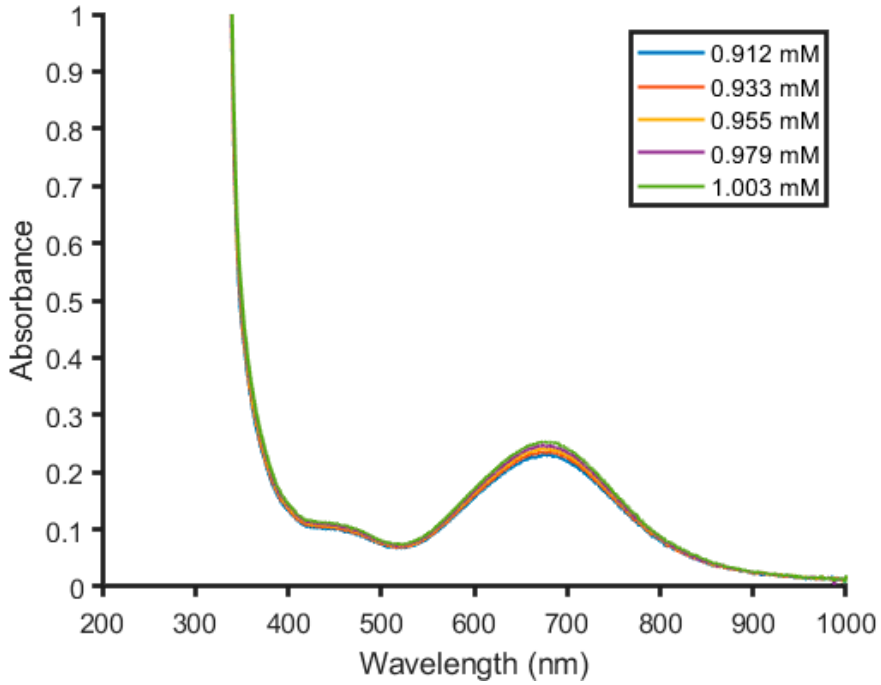

Figure S15 Beer's law analysis of $^{3}[Cu_2Cl_2]^{2+}$ at 676 nm.

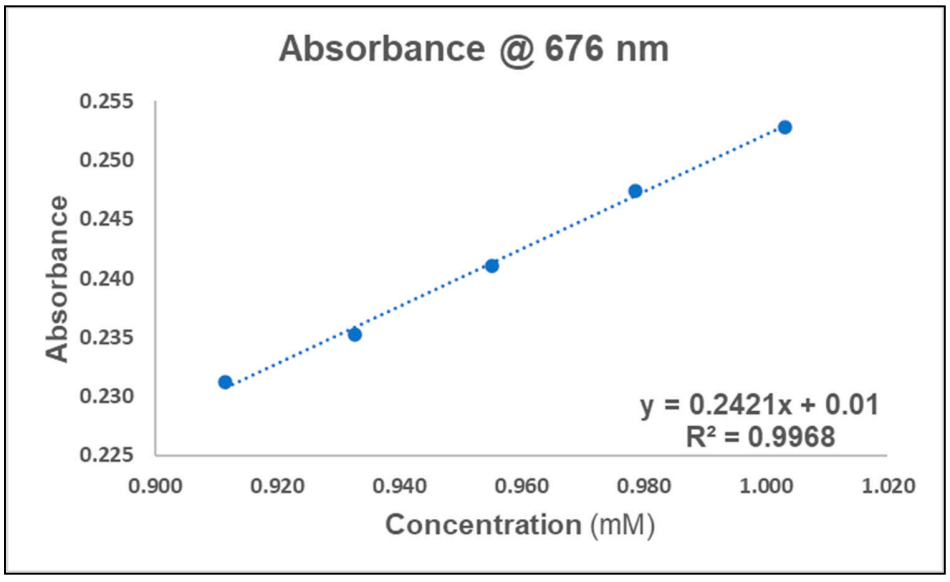

Figure S16 Linear fit of $^{3}[Cu_2Cl_2]^{2+}$ absorbance data at 676 nm.

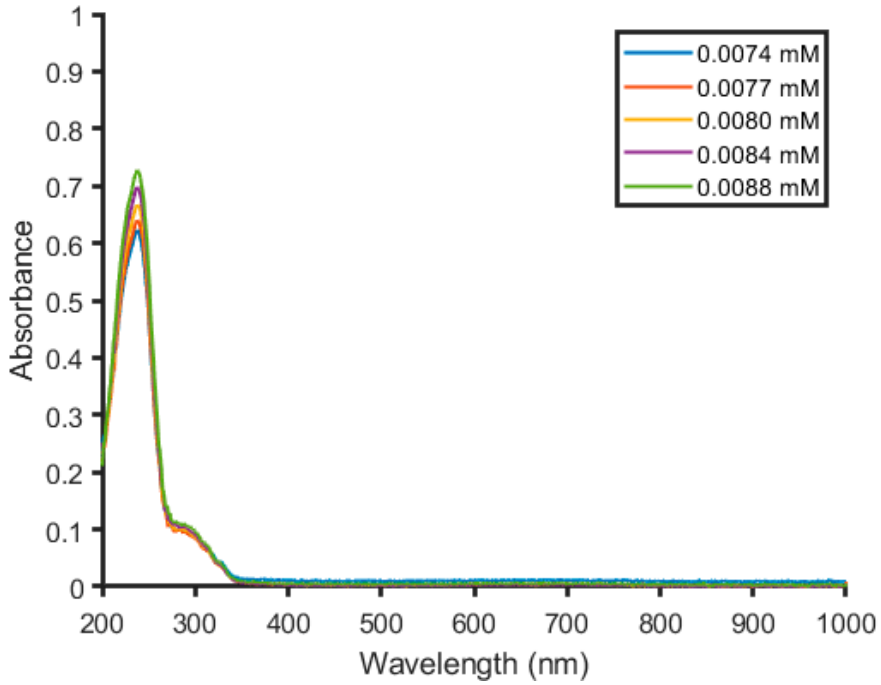

Figure S17 Beer's law analysis of $^{3}[Cu_2Cl_2]^{2+}$ at 238 nm.

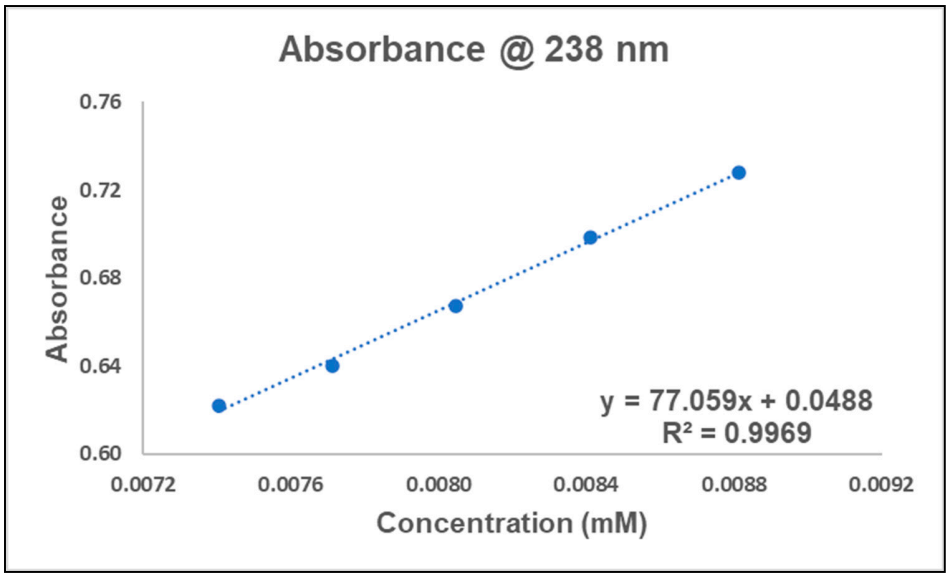

Figure S18 Linear fit of $^{3}[Cu_2Cl_2]^{2+}$ absorbance data at 238 nm.

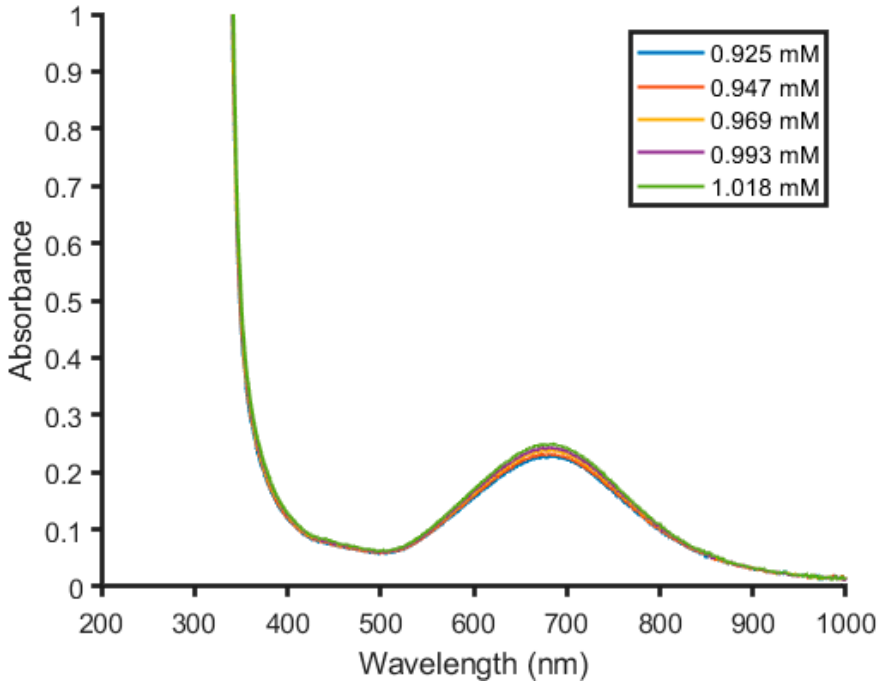

Figure S19 Beer's law analysis of $^{2}[Cu_2Cl_2]^{2+}$ at 681 nm.

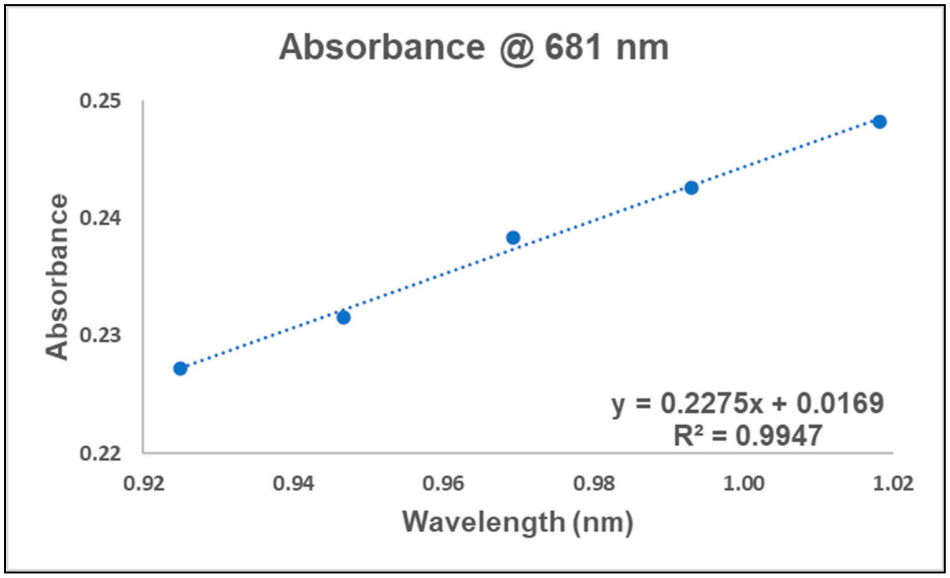

Figure S20 Linear fit of $^{3}[Cu_2Cl_2]^{2+}$ absorbance data at 681 nm.

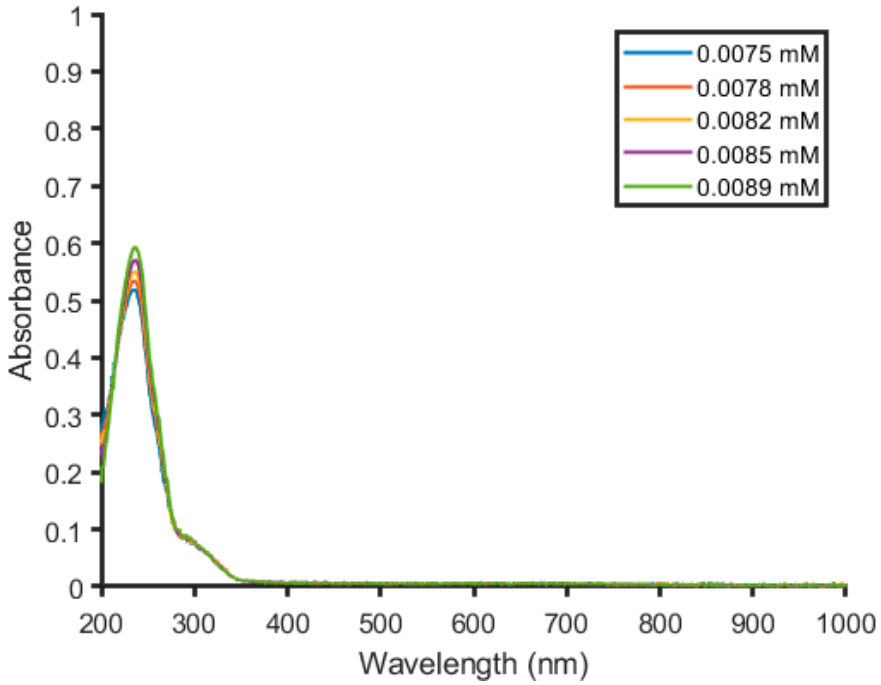

Figure S21 Beer's law analysis of $^{2}[Cu_2Cl_2]^{2+}$ at 236 nm.

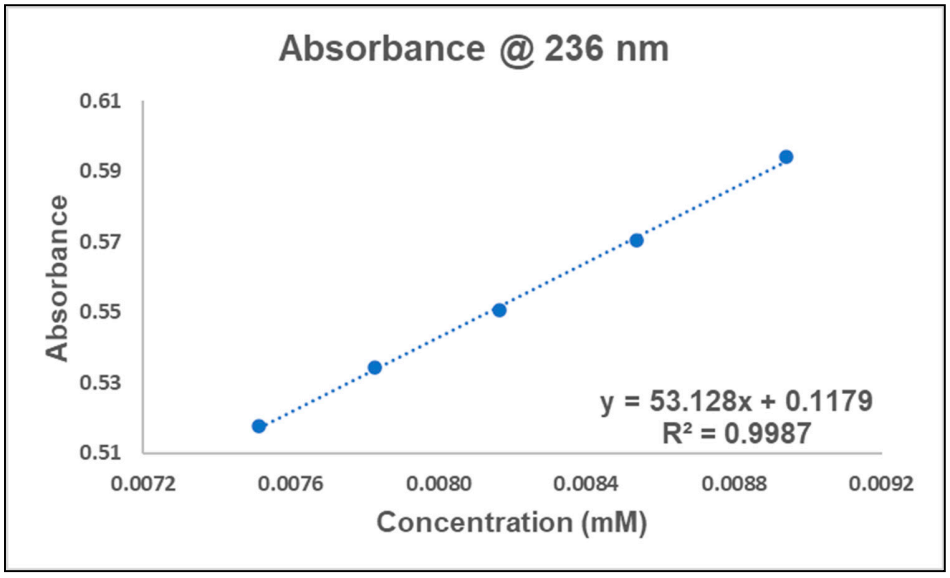

Figure S22 Linear fit of $^{2}[Cu_2Cl_2]^{2+}$ absorbance data at 236 nm.

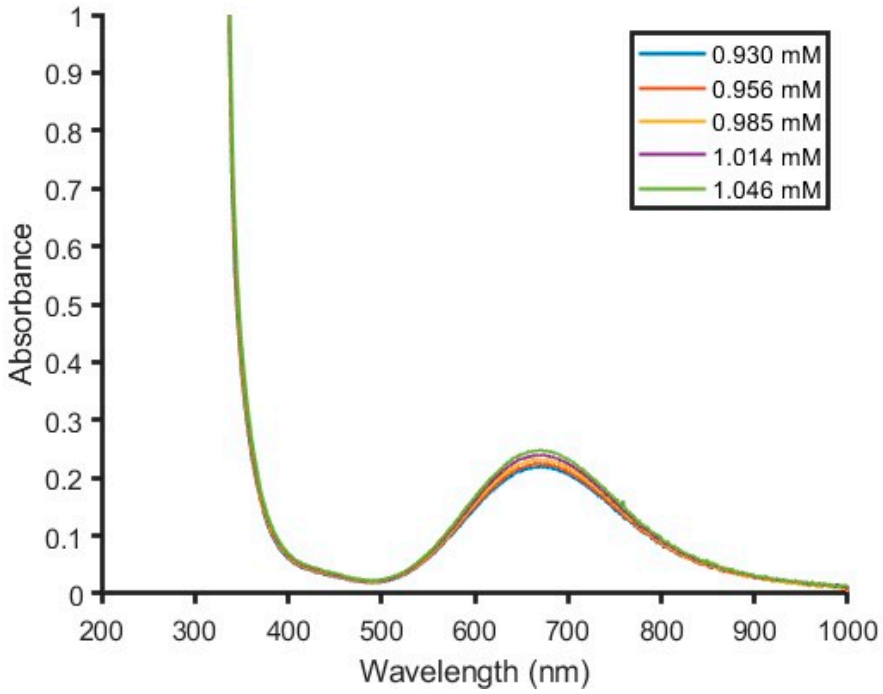

Figure S23 Beer's law analysis of $^{3}[Cu_2F]^{3+}$ at 667 nm.

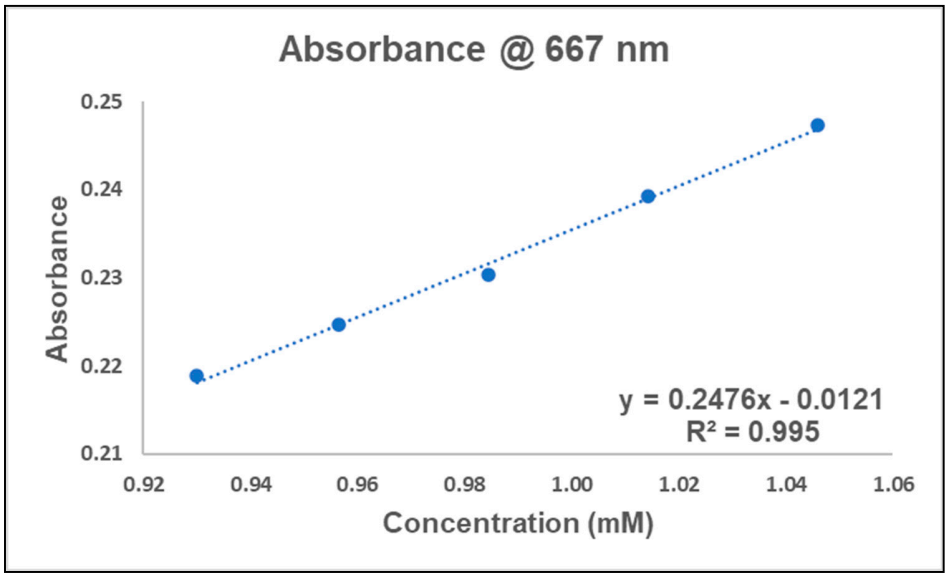

Figure S24 Linear fit of $^{3}[Cu_2F]^{3+}$ absorbance data at 667 nm.

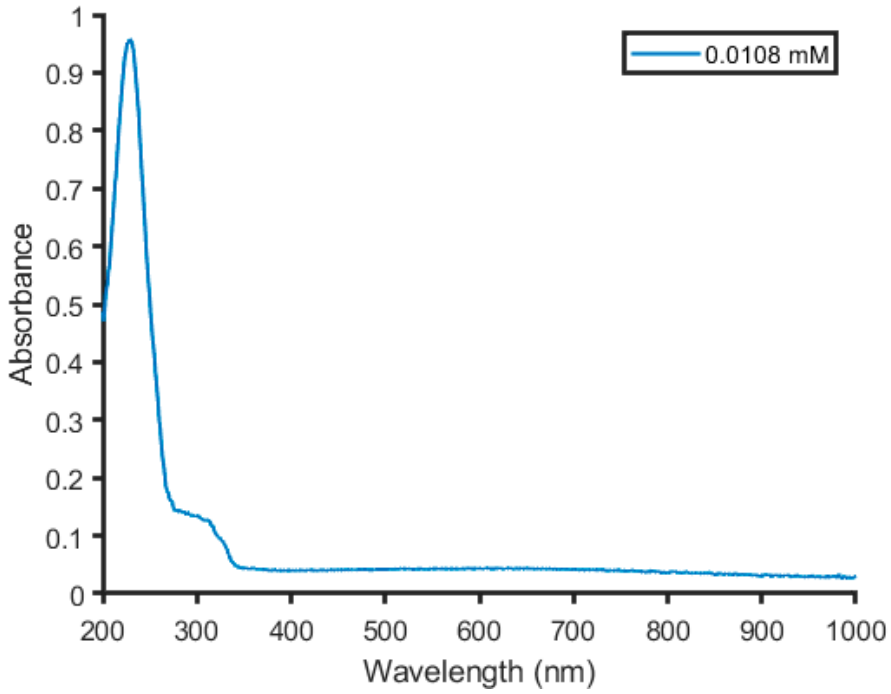

Figure S25 Representative example of ^{3}**[Cu$_2$F]$^{3+}$** π-π* transition at 230 nm.

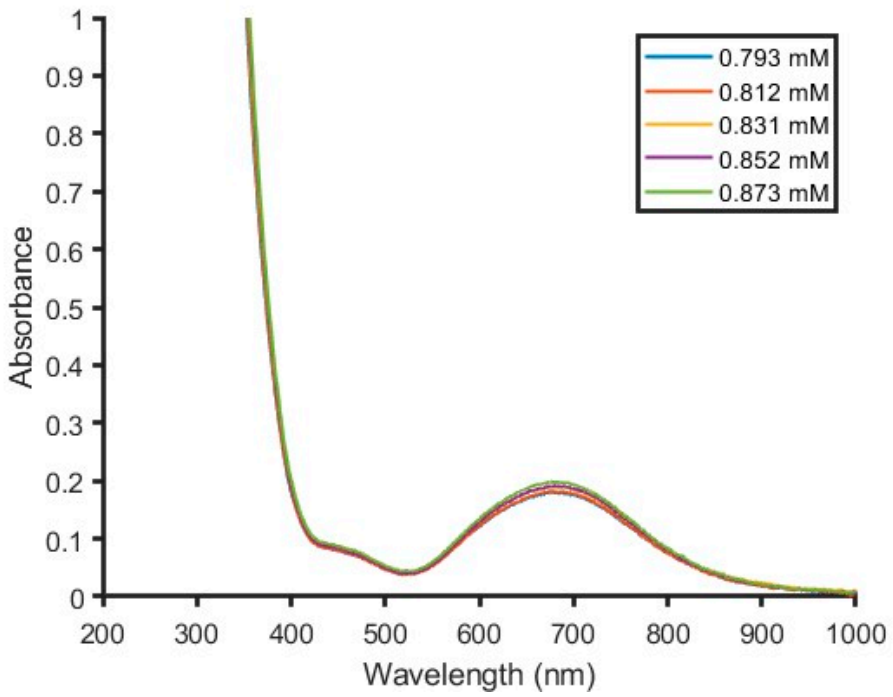

Figure S26 Beer's law analysis of $^{3}[Cu_2Br_2]^{2+}$ 679 nm.

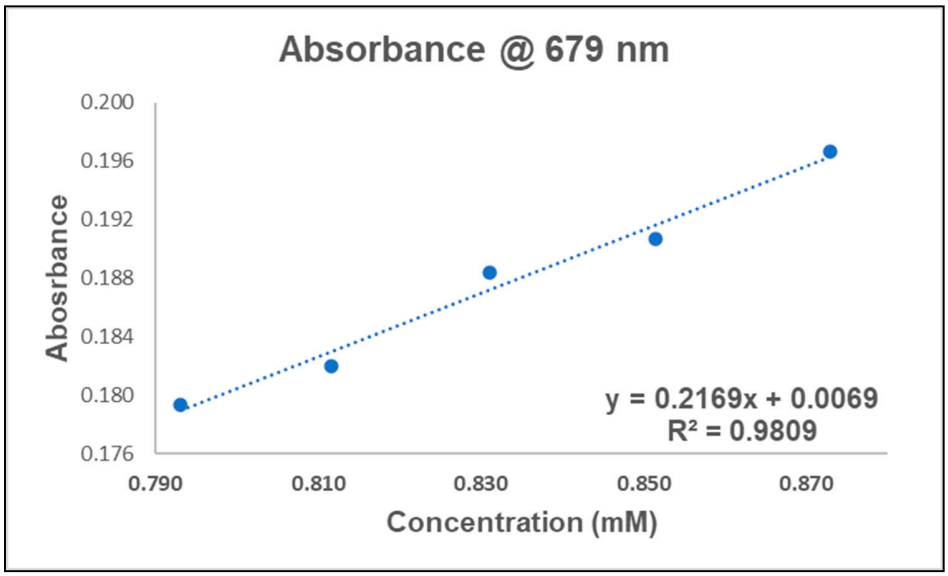

Figure S27 Linear fit of $^{3}[Cu_2Br_2]^{2+}$ absorbance data at 679 nm.

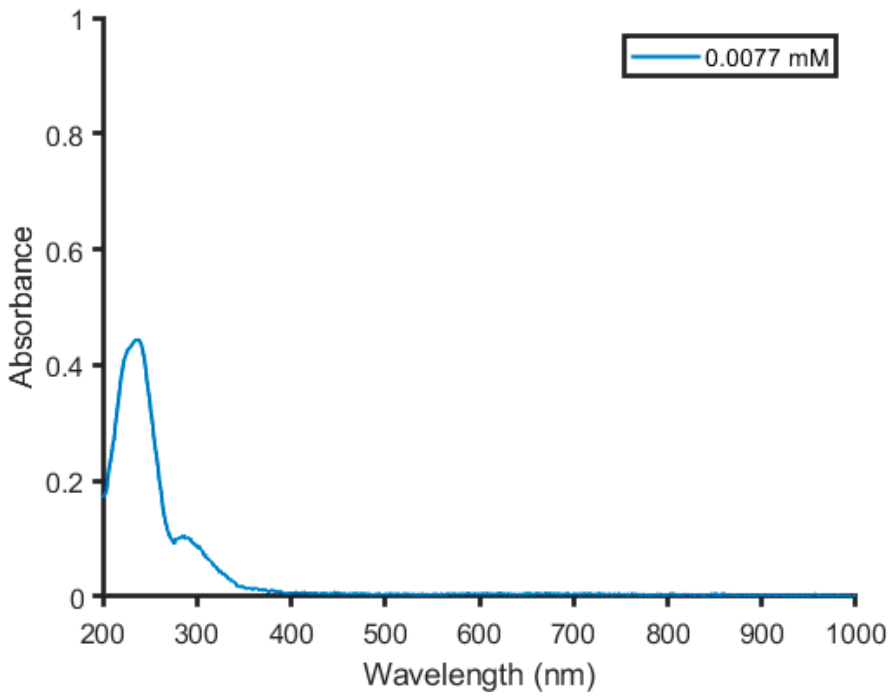

Figure S28 Representative example of $^{3}[Cu_2Br_2]^{3+}$ π-π* transition at 236 nm.

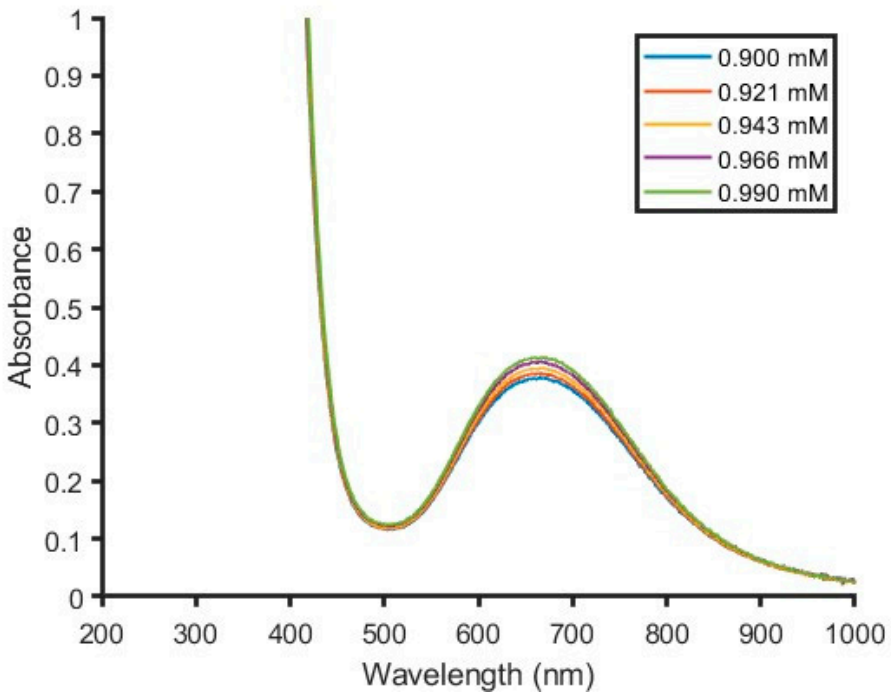

Figure S29 Beer's law analysis of $^{3}[Cu_2(N_3)_2]^{2+}$ at 661 nm.

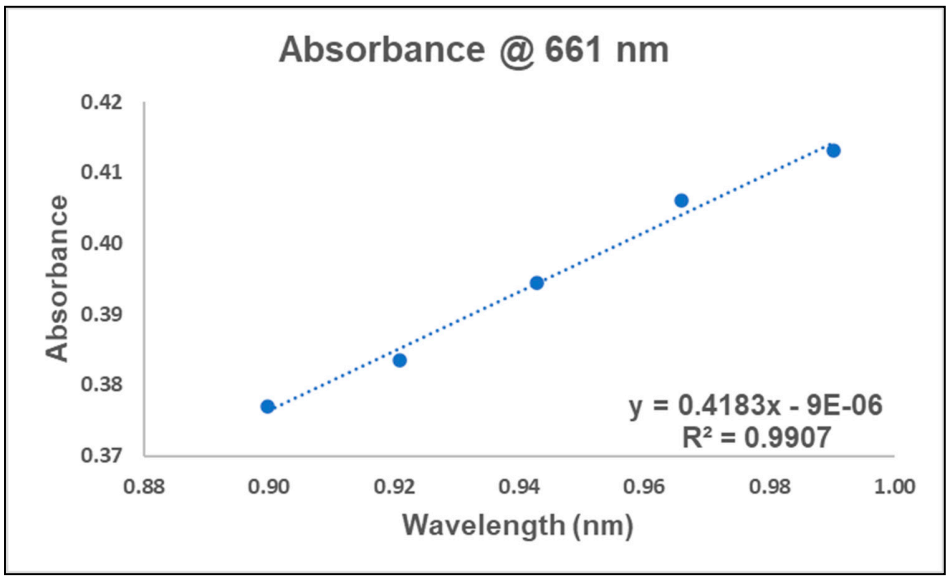

Figure S30 Linear fit of $^{3}[Cu_2(N_3)_2]^{2+}$ absorbance data at 661 nm.

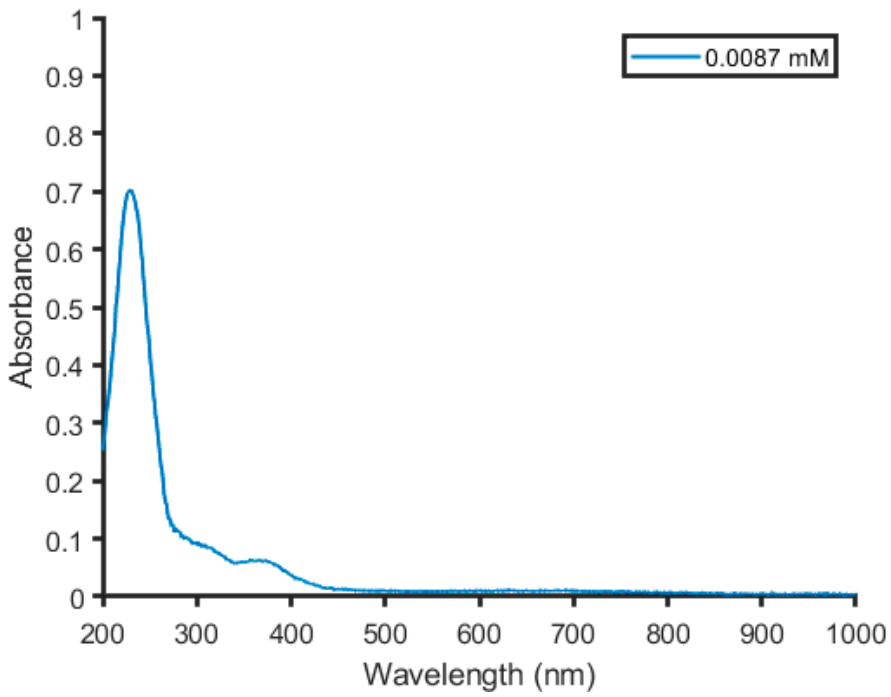

Figure S31 Representative example of $^{3}[Cu_2(N_3)_2]^{2+}$ π-π* transition at 229 nm.

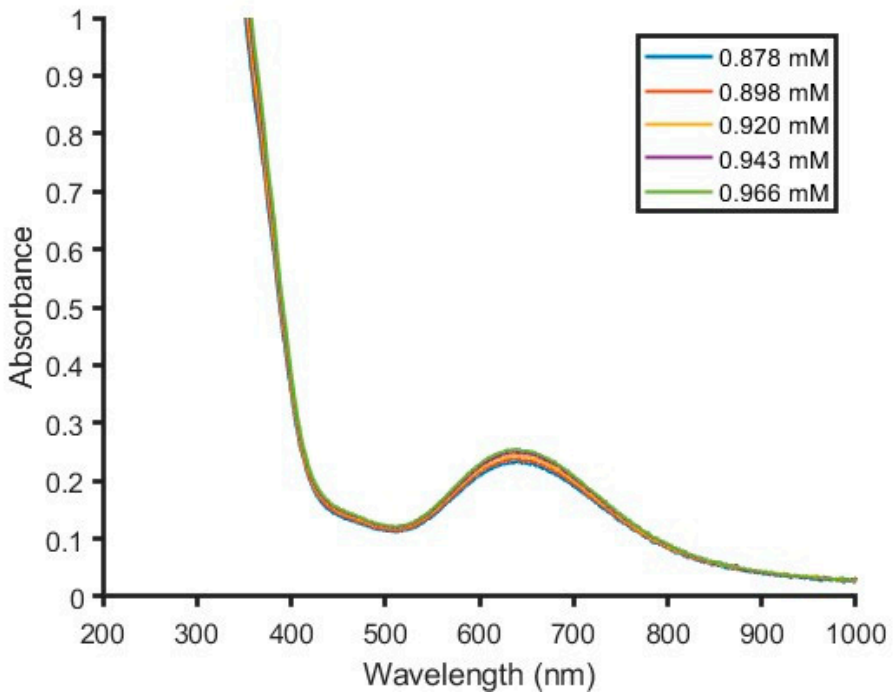

Figure S32 Beer's law analysis of $^{3}[Cu_2(ONO)_2]^{2+}$ at 638 nm.

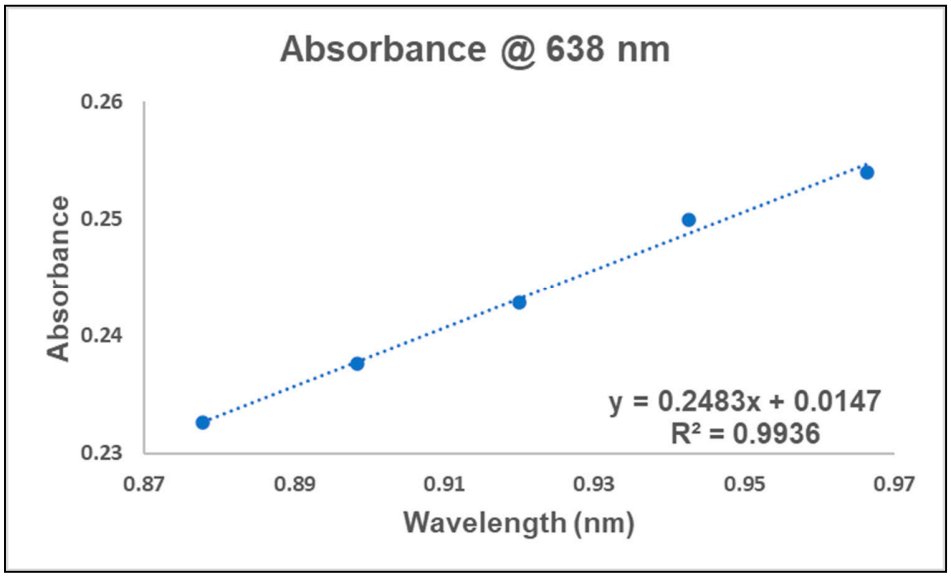

Figure S33 Linear fit of $^{3}[Cu_2(ONO)_2]^{2+}$ absorbance data at 638 nm.

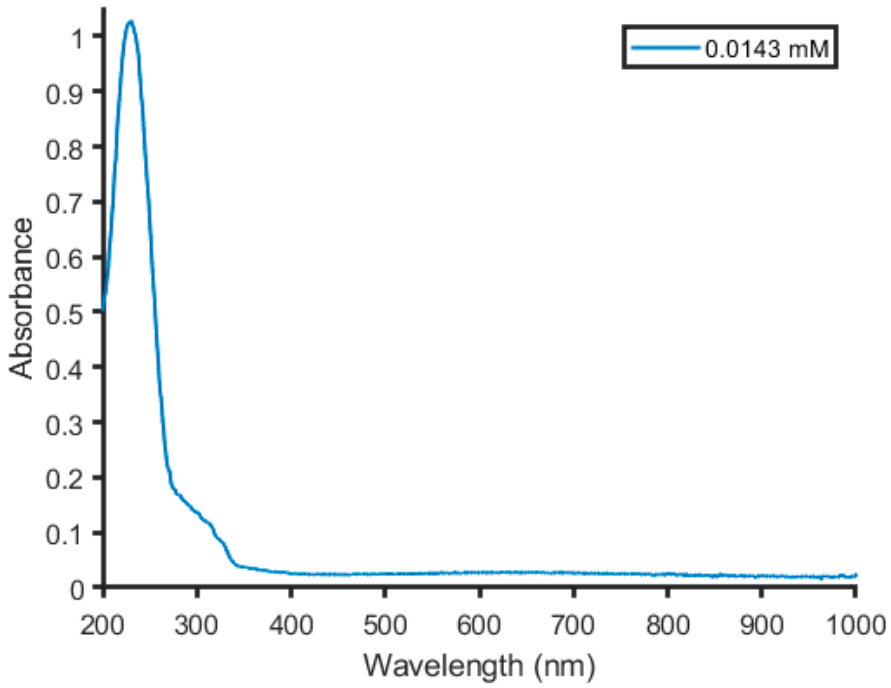

Figure S34 Representative example of $^{3}[Cu_2(ONO)_2]^{2+}$ π-π* transition at 230 nm.

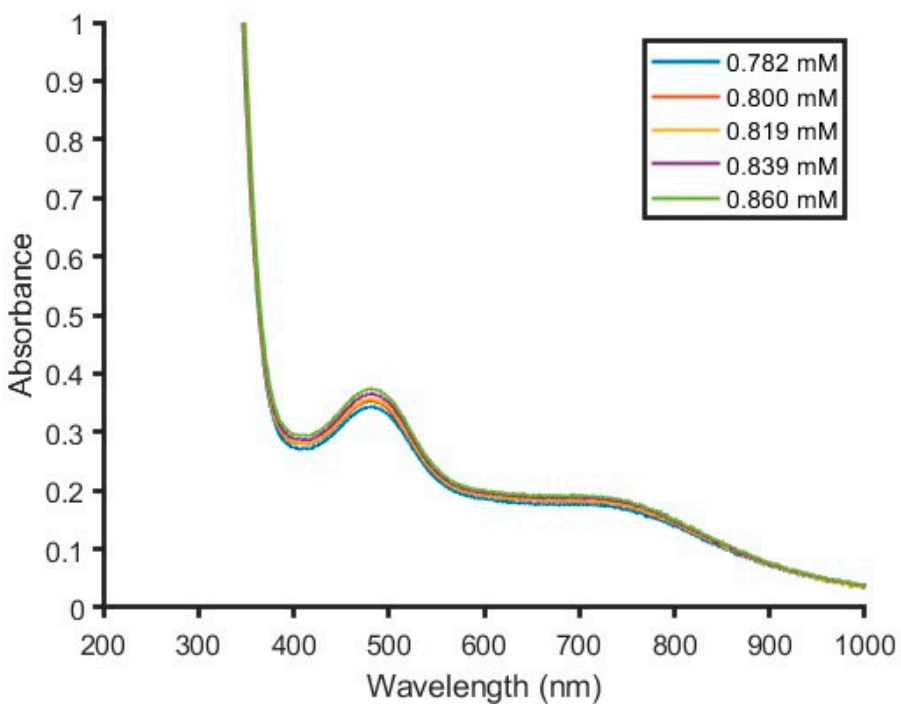

Figure S35 Beer's law analysis of $^{3}[Cu_2(OTMS)_2]^{2+}$ at 481 nm.

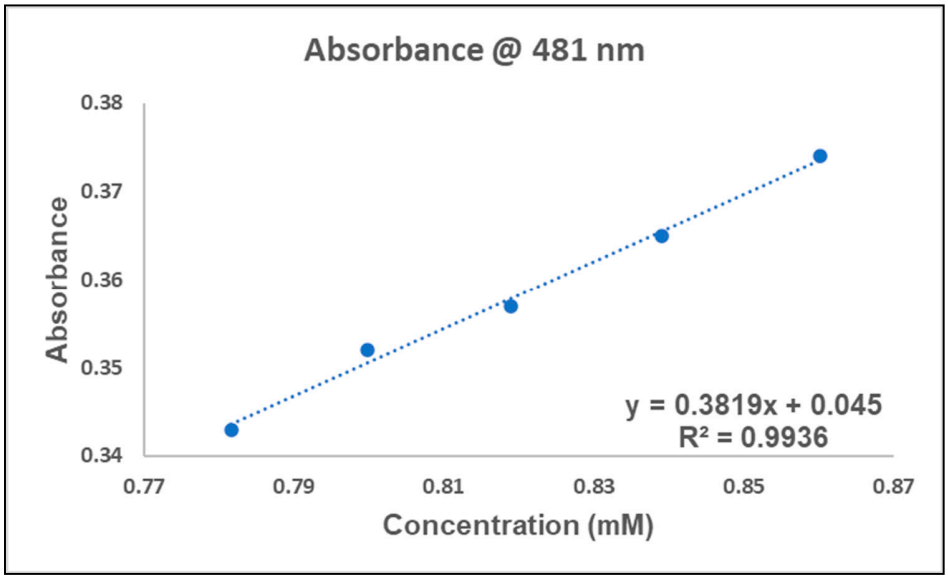

Figure S36 Linear fit of $^{3}[Cu_2(OTMS)_2]^{2+}$ absorbance data at 481 nm.

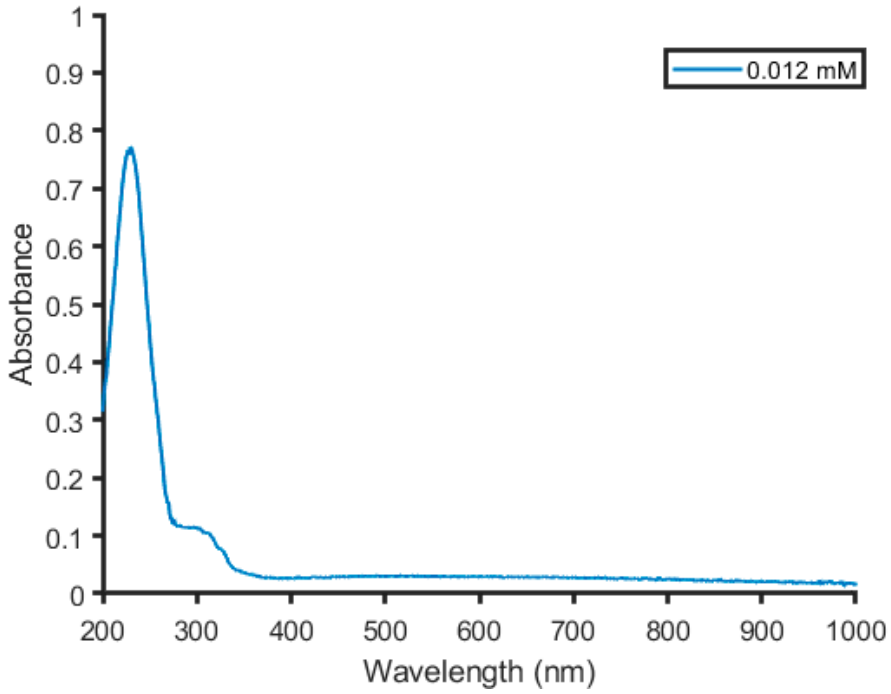

Figure S37 Representative example of ^{3}**[Cu$_2$(OTMS)$_2$]$^{2+}$** π-π* transition at 229 nm.

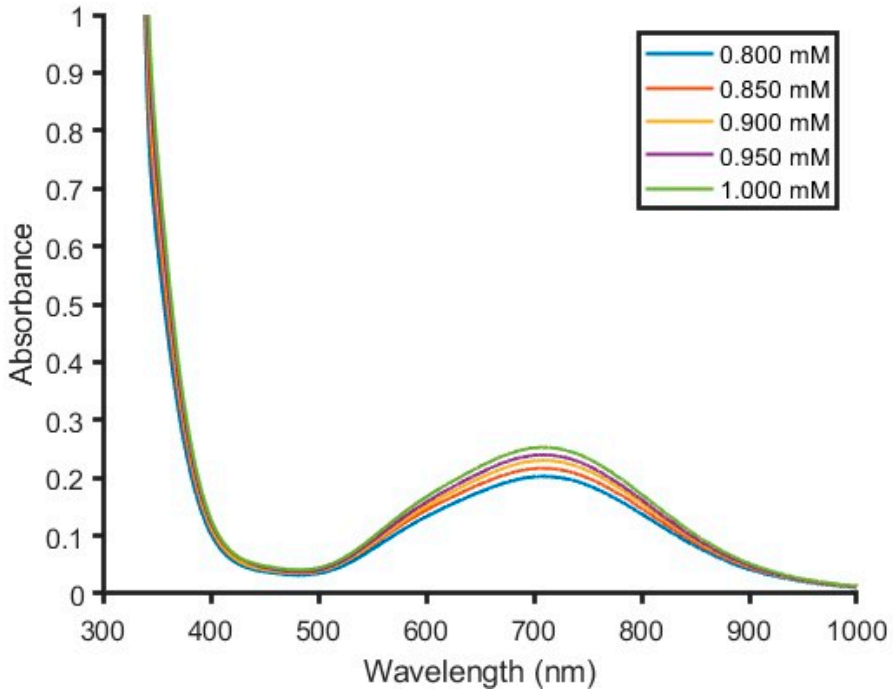

Figure S38 Beer's law analysis of $^{3}[Cu_2OH]^{3+}$ absorbance data at 708 nm.

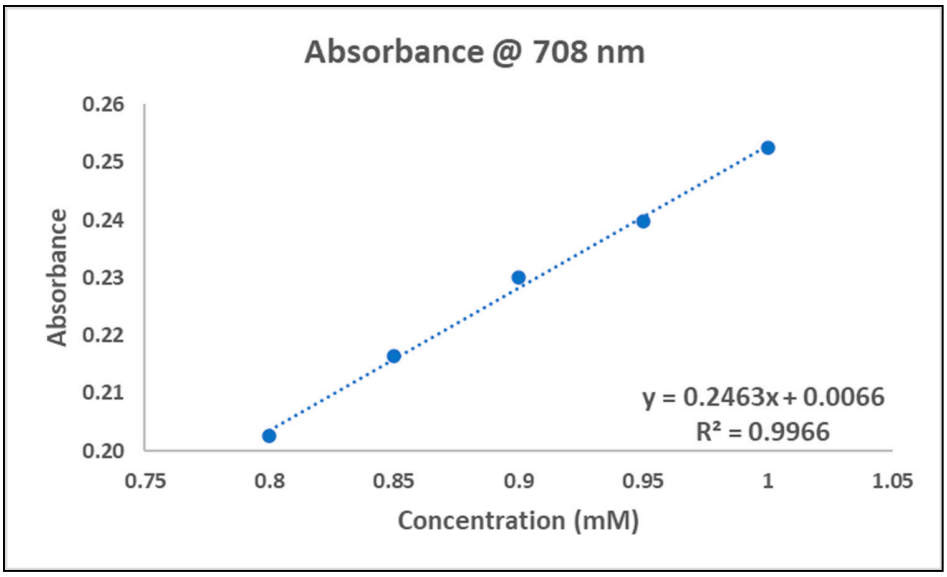

Figure S39 Linear fit of $^{3}[Cu_2OH]^{3}$ absorbance data at 708 nm.

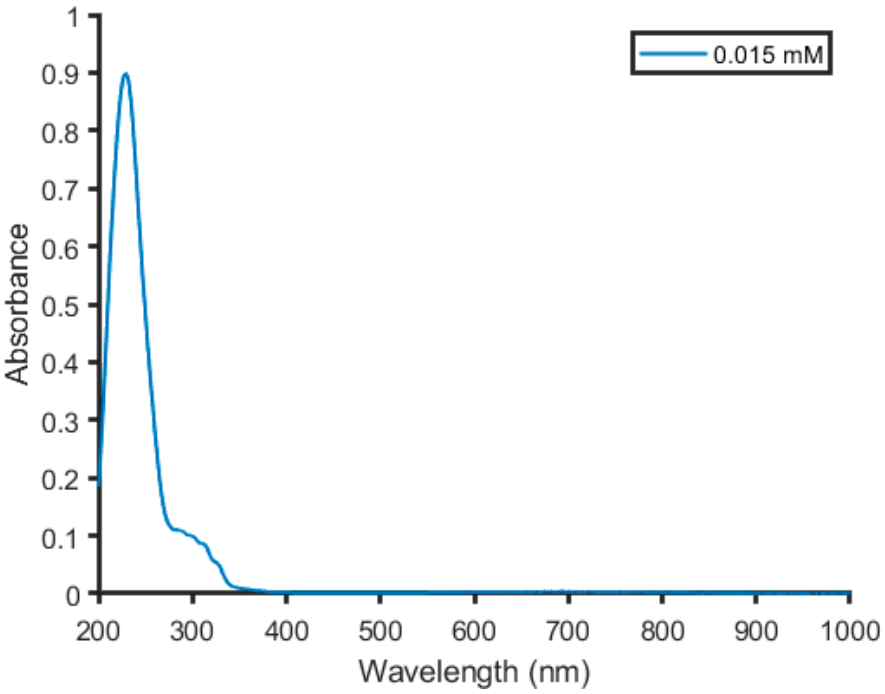

Figure S40 Representative example of ^{3}**[Cu$_2$OH]$^{3+}$** π-π* transition at 229 nm.

IV. X-ray Crystallography

Table S1 Summary of structure determination of **$^{3}[Cu_2Cl_2]^{2+}$**.

Empirical formula	$C_{34}H_{46}Cl_2Cu_2F_6N_6O_6S_2$
Formula weight	1010.87
Temperature/K	100
Crystal system	monoclinic
Space group	$P2_1/c$
a	12.5444(7)Å
b	15.9671(9)Å
c	11.8223(7)Å
β	117.009(2)°
Volume	2109.7(2)Å^3
Z	2
d_{calc}	1.591 g/cm^3
μ	1.310 mm^{-1}
F(000)	1036.0
Crystal size, mm	0.3 × 0.2 × 0.02
2θ range for data collection	6.272 - 55.24°
Index ranges	-16 ≤ h ≤ 16, -20 ≤ k ≤ 20, -15 ≤ l ≤ 15
Reflections collected	51161
Independent reflections	4881[R(int) = 0.0957]
Data/restraints/parameters	4881/84/339
Goodness-of-fit on F^2	1.051
Final R indexes (I>=2σ (I))	R_1 = 0.0728, wR_2 = 0.1776
Final R indexes (all data)	R_1 = 0.0970, wR_2 = 0.1998
Largest diff. peak/hole	1.03/-1.28 eÅ^{-3}

Table S2 Summary of structure determination of $^{2}[Cu_2Cl_2]^{2+}$.

Empirical formula	$C_{36}H_{48}Cl_2Cu_2F_6N_8O_6S_2$
Formula weight	1064.92
Temperature/K	100
Crystal system	triclinic
Space group	$P\bar{1}$
a	12.6430(12)Å
b	13.7270(13)Å
c	28.579(3)Å
α	79.827(3)°
β	82.354(3)°
γ	68.329(3)°
Volume	4524.4(7)Å^3
Z	4
d_{calc}	1.563 g/cm^3
μ	1.228 mm^{-1}
F(000)	2184.0
Crystal size, mm	0.38 × 0.32 × 0.25
2θ range for data collection	5.772 - 55.138°
Index ranges	-16 ≤ h ≤ 16, -17 ≤ k ≤ 17, -37 ≤ l ≤ 37
Reflections collected	108801
Independent reflections	20849[R(int) = 0.0472]
Data/restraints/parameters	20849/0/1142
Goodness-of-fit on F^2	1.023
Final R indexes (I>=2σ (I))	R_1 = 0.0664, wR_2 = 0.2072
Final R indexes (all data)	R_1 = 0.0739, wR_2 = 0.2203
Largest diff. peak/hole	1.15/-0.69 eÅ^{-3}

Table S3 Summary of structure determination of $^{3}[Cu_2(NCMe)_2]^{4+}$.

Empirical formula	$C_{44}H_{58}Cu_2F_{12}N_{10}O_{12}S_4$
Formula weight	1402.32
Temperature/K	100
Crystal system	triclinic
Space group	$P\bar{1}$
a	9.5549(3)Å
b	12.0215(4)Å
c	13.3759(4)Å
α	103.747(2)°
β	105.331(3)°
γ	91.855(2)°
Volume	1431.84(8)Å^3
Z	1
d_{calc}	1.626 g/cm^3
μ	3.224 mm^{-1}
F(000)	718.0
Crystal size, mm	0.11 × 0.04 × 0.03
2θ range for data collection	7.088 - 148.932°
Index ranges	-11 ≤ h ≤ 11, -12 ≤ k ≤ 15, -16 ≤ l ≤ 16
Reflections collected	18204
Independent reflections	5765[R(int) = 0.0476]
Data/restraints/parameters	5765/0/386
Goodness-of-fit on F^2	1.074
Final R indexes (I>=2σ (I))	R_1 = 0.0520, wR_2 = 0.1434
Final R indexes (all data)	R_1 = 0.0628, wR_2 = 0.1567
Largest diff. peak/hole	0.66/-0.85 eÅ^{-3}

Table S4 Summary of structure determination of ^{3}**[Cu$_2$Cl]$^{3+}$**.

Empirical formula	$C_{35}H_{46}ClCu_2F_9N_6O_9S_3$
Formula weight	1124.49
Temperature/K	100
Crystal system	monoclinic
Space group	$P2_1/n$
a	15.4647(5)Å
b	11.5756(4)Å
c	25.5577(6)Å
β	96.493(3)°
Volume	4545.8(2)Å^3
Z	4
d_{calc}	1.643 g/cm^3
μ	1.227 mm^{-1}
F(000)	2296.0
Crystal size, mm	0.46 × 0.16 × 0.06
2θ range for data collection	4.584 - 56.564°
Index ranges	-20 ≤ h ≤ 20, -15 ≤ k ≤ 15, -32 ≤ l ≤ 34
Reflections collected	79844
Independent reflections	11270[R(int) = 0.0508]
Data/restraints/parameters	11270/216/651
Goodness-of-fit on F^2	1.033
Final R indexes (I>=2σ (I))	R_1 = 0.0485, wR_2 = 0.1237
Final R indexes (all data)	R_1 = 0.0618, wR_2 = 0.1309
Largest diff. peak/hole	1.53/-0.75 eÅ^{-3}

Table S5 Summary of structure determination of $^{3}[Cu_2F]^{3+}$.

Empirical formula	$C_{35}H_{46}Cu_2F_{10}N_6O_9S_3$
Formula weight	1108.04
Temperature/K	100
Crystal system	monoclinic
Space group	P2/c
a	13.7556(5)Å
b	9.1159(3)Å
c	17.8988(6)Å
β	103.059(4)°
Volume	2186.37(13)Å^3
Z	2
d_{calc}	1.683 g/cm^3
μ	1.218 mm^{-1}
F(000)	1132.0
Crystal size, mm	0.44 × 0.14 × 0.08
2θ range for data collection	4.672 - 56.564°
Index ranges	-18 ≤ h ≤ 17, -10 ≤ k ≤ 12, -23 ≤ l ≤ 23
Reflections collected	42756
Independent reflections	5424[R(int) = 0.0553]
Data/restraints/parameters	5424/0/336
Goodness-of-fit on F^2	1.035
Final R indexes [I>=2σ (I)]	R_1 = 0.0430, wR_2 = 0.1037 Final
R indexes (all data)	R_1 = 0.0510, wR_2 = 0.1077
Largest diff. peak/hole	1.88/-1.11 eÅ^{-3}

Table S6 Summary of structure determination of $^{3}[Cu_2(N_3)_2]^{2+}$.

Empirical formula	$C_{34}H_{46}Cu_2F_6N_{12}O_6S_2$
Formula weight	1024.03
Temperature/K	100
Crystal system	monoclinic
Space group	$P2_1/c$
a	7.6454(2)Å
b	12.0716(2)Å
c	23.2817(5)Å
β	94.729(2)°
Volume	2141.41(8)Å^3
Z	2
d_{calc}	1.588 g/cm^3
μ	1.175 mm^{-1}
F(000)	1052.0
Crystal size, mm	0.18 × 0.17 × 0.12
2θ range for data collection	3.804 - 56.562°
Index ranges	-10 ≤ h ≤ 9, -16 ≤ k ≤ 16, -31 ≤ l ≤ 31
Reflections collected	42276
Independent reflections	5301[R(int) = 0.0338]
Data/restraints/parameters	5301/0/285
Goodness-of-fit on F^2	1.042
Final R indexes [I>=2σ (I)]	R_1 = 0.0236, wR_2 = 0.0610 Final
R indexes (all data)	R_1 = 0.0262, wR_2 = 0.0621
Largest diff. peak/hole	0.42/-0.32 eÅ^{-3}

Table S7 Summary of structure determination of $^{3}[Cu_2(ONO)_2]^{2+}$

Empirical formula	$C_{34}H_{46}Cu_2F_6N_8O_{10}S_2$
Formula weight	1031.99
Temperature/K	100
Crystal system	monoclinic
Space group	$P2_1/c$
a	8.1673(3)Å
b	11.6841(4)Å
c	23.3957(7)Å
β	98.843(3)°
Volume	2206.06(13)Å^3
Z	2
d_{calc}	1.554 g/cm^3
μ	1.145 mm^{-1}
F(000)	1060.0
Crystal size, mm	0.26 × 0.16 × 0.09
2θ range for data collection	4.958 - 56.56°
Index ranges	-10 ≤ h ≤ 10, -15 ≤ k ≤ 15, -31 ≤ l ≤ 30
Reflections collected	40925
Independent reflections	5463[R(int) = 0.0814]
Data/restraints/parameters	5463/18/294
Goodness-of-fit on F^2	1.066
Final R indexes (I>=2σ (I))	R_1 = 0.0304, wR_2 = 0.0745
Final R indexes (all data)	R_1 = 0.0373, wR_2 = 0.0772
Largest diff. peak/hole	0.45/-0.45 eÅ^{-3}

Table S8 Summary of structure determination of $^{3}[Cu_2(OTMS)_2]^{2+}$

Empirical formula	$C_{20}H_{32}CuF_3N_3O_4SSi$
Formula weight	559.17
Temperature/K	100
Crystal system	monoclinic
Space group	$P2_1/n$
a	13.8850(14)Å
b	13.0849(13)Å
c	15.4405(15)Å
β	114.690(2)°
Volume	2548.8(4)Å^3
Z	4
d_{calc}	1.457 g/cm^3
μ	1.038 mm^{-1}
F(000)	1164.0
Crystal size, mm	0.3 × 0.25 × 0.2
2θ range for data collection	4.484 - 55.018°
Index ranges	-18 ≤ h ≤ 17, -16 ≤ k ≤ 17, -20 ≤ l ≤ 20
Reflections collected	46045
Independent reflections	5846[R(int) = 0.0188]
Data/restraints/parameters	5846/18/306
Goodness-of-fit on F^2	1.039
Final R indexes (I>=2σ (I))	R_1 = 0.0373, wR_2 = 0.0967
Final R indexes (all data)	R_1 = 0.0405, wR_2 = 0.0995
Largest diff. peak/hole	1.32/-1.22 eÅ^{-3}

Table S9 Summary of structure determination of ^{3}**[Cu$_2$OH]$^{3+}$**.

Empirical formula	$C_{39}H_{55}Cu_2F_9N_6O_{11}S_3$
Formula weight	1178.15
Temperature/K	100
Crystal system	triclinic
Space group	$P\bar{1}$
a	12.1466(12)Å
b	14.6587(16)Å
c	14.8914(16)Å
α	67.013(4)°
β	81.872(4)°
γ	83.338(4)°
Volume	2411.0(4)Å^3
Z	2
d_{calc}	1.623 g/cm^3
μ	1.110 mm^{-1}
F(000)	1212.0
Crystal size, mm	0.41 × 0.33 × 0.05
2θ range for data collection	5.976 - 55.158°
Index ranges	-15 ≤ h ≤ 15, -19 ≤ k ≤ 19, -19 ≤ l ≤ 19
Reflections collected	67617
Independent reflections	11091[R(int) = 0.0686]
Data/restraints/parameters	11091/259/753
Goodness-of-fit on F^2	1.127
Final R indexes (I>=2σ (I))	R_1 = 0.0564, wR_2 = 0.0903
Final R indexes (all data)	R_1 = 0.0800, wR_2 = 0.0977
Largest diff. peak/hole	0.94/-0.59 eÅ^{-3}